

# Velocity Decomposition Analysis of Free Surface Flow

Paul F. White, Yang Chen, Kevin J. Maki, and Robert F. Beck

Department of Naval Architecture and Marine Engineering  
University of Michigan, Ann Arbor, MI, 48109 USA  
pfwhite@umich.edu

## INTRODUCTION

Computational Fluid Dynamics (CFD) has become increasingly used as a design tool for ships and offshore structures. Although CFD captures more relevant physics than traditional Boundary Element Methods (BEM), the improved accuracy comes at a cost. CFD simulations are both computationally intensive and time consuming to complete. One subset of research in the field of CFD has been devoted to developing more efficient CFD methods while not sacrificing features that give CFD its advantage.

Two methods that attempt to increase the computational efficiency of CFD are domain decomposition methods[1] and velocity decomposition methods [2, 4, 6]. The domain decomposition method aims to reduce the size of the CFD mesh to a small region that includes the body and all of the rotational flow. The so-called matching boundary surrounds this small inner region and serves as the outer boundary of the CFD computational domain. Outside this region the flow is assumed to be potential. Far from the body the potential flow must satisfy the usual boundary conditions at infinity. On the matching boundary the inner boundary conditions on the potential flow are coupled to the outer boundary of the viscous-flow solution and the problem is solved in an iterative fashion.

In the velocity decomposition method a Helmholtz-type velocity decomposition is used to break the total velocity field into the sum of an irrotational component (the viscous potential flow) and a rotational component (the vortical flow). The vortical flow is found using a conventional CDF solver. The viscous potential is found using a potential-flow solver, for instance a panel method, in conjunction with a modified body boundary condition that accounts for the influence of the viscous flow on the far-field potential flow. The viscous potential in turn sets the boundary conditions on the outer edges of the CFD computational domain. Because of this interaction, the size of the CFD computational domain can be greatly reduced (in principle it only has to include the rotational flow region) resulting in a significant savings in computational time.

The long-term goal of the research is to develop a method that uses the viscous potential in free surface flows to greatly reduce the size of the viscous flow computational domain and thus significantly reduce the computational time. The work reported in this paper starts with double-body flow [2, 3] and progresses to the Wigley hull with a free surface.

## METHOD

The velocity field  $\mathbf{u}$  is decomposed into a irrotational component represented by the viscous potential  $\varphi$  and a vortical velocity  $\mathbf{w}$ :

$$\mathbf{u}(\mathbf{x}, t) = \nabla\varphi(\mathbf{x}, t) + \mathbf{w}(\mathbf{x}, t). \quad (1)$$

The total velocity on the reduced domain is found using a flow solver based on the OpenFOAM opensource CFD library. The viscous potential is determined with the higher-order boundary element solver Aegir[5]. The coupling condition is a relation between the normal component of the viscous potential on the body and the normal component of the vortical velocity on the body. Following the details of [2, 6], an iterative procedure is developed to calculate the modified viscous-body-boundary condition for the BEM solver. The iterative condition is:

$$\frac{\partial\varphi^{(i+1)}}{\partial n} = \frac{\partial\varphi^{(i)}}{\partial n} + w_n^{(i)}(\delta). \quad (2)$$

where  $w_n$  is the body-normal component of the vortical velocity evaluated at a distance  $\delta$  from the body.  $\delta$  is the normal distance from the body where the vorticity falls to a negligible value. At each intermediate iteration,  $i$ , the vortical velocity is recalculated by taking the difference between the CFD field solution and the viscous potential velocity. As the algorithm converges the normal component of the vortical velocity at the edge of the viscous region approaches zero.

**Double-Body Method** The double-body problem is solved on a Wigley hull at Reynolds number of  $4 \times 10^6$ . This corresponds to a  $L = 4$  m in water. A CFD solver from OpenFOAM is used on a domain that extends  $0.05L$  from the body on the sides and upstream, and  $1L$  downstream from the transom. The solution for the double-body problem is denoted  $\mathbf{u}_{db}$  and  $\varphi_{db}$ .

**Preliminary Free-Surface Flow Method** As previously stated the ultimate goal of this work is to develop a procedure to find a viscous potential that will allow for drastic reduction in the dimension of the CFD domain. At the present time of writing, we have made the first steps towards this goal. We start with the computation of the total solution on a large domain with a volume-of-fluid CFD solver. From this solution we can identify the extent of the rotational region and calculate the function  $\delta(\mathbf{x}_b)$ . At this stage, we solve for a viscous potential using the double-body domain but with a modified body-boundary condition based on the total velocity at the extent of the rotational region. We denote this solution  $\varphi'$  because it is an approximation to the complete viscous potential. In other words, it is a double-body potential with rotational flow effects that also see the influence of the wave field. The only difference between the  $\varphi_{db}$  and  $\varphi'$  is that the later uses a velocity field from the wave solution to specify the modified boundary condition.

## RESULTS

The results are expressed in a coordinate system with  $x$  upstream and  $y$  downward. The origin is at midships, calm-water plane and centerline.

**Double-Body Results** For the double-body results a large-eddy simulation method is used. Figure 1 shows the BEM discretization and the value of the normal component of the viscous potential on the hull surface and the wake. The top of this figure shows the normal component of the total viscous potential velocity. In the bottom the difference between the normal component of the total viscous potential and the inviscid potential velocities is shown. This difference is labeled the transpiration velocity  $v_{tr}$ . Note that the transpiration velocity is less than several percent of the total free-stream velocity value over the forward portion of the hull, whereas in the stern it is near ten percent of the free-stream value. For the Wigley hull at this Reynolds number the flow remains attached, yet, the boundary layers on the hull grow substantially near the stern and the thickness of the viscous wake is approximately that of the beam behind the body.

The double-body flow is shown in Figure 2. On the top right contours of dimensionless vorticity are shown. The colored area represents where the velocity is rotational, and in principle only this region must be discretized with the CFD method. On the top left contours of the dimensionless vortical velocity are shown. This quantity is defined as  $\mathbf{w}^* = (\mathbf{u}_{db} - \nabla\varphi_{db})/U_\infty$ . Note the similarity in the extent of the colored region in both the vortical velocity and the vorticity plots. If the vortical velocity is zero outside of the rotational region, then the viscous potential can be used for the Dirichlet boundary conditions for the total velocity on the extent of the reduced domain. Finally, for reference, the dimensionless vortical velocity that is calculated using the inviscid potential as shown in the bottom of this figure. Here  $\mathbf{w}_{inv}^* = (\mathbf{u}_{db} - \nabla\phi_{db})/U_\infty$ , where  $\phi_{db}$  is the inviscid potential that satisfies the no-penetration condition on the body. Note how the colored region is larger. This means the CFD domain must be larger if the inviscid potential velocity is to be used as a Dirichlet boundary condition for the total velocity on its extents.

To examine the convergence of the iterative algorithm velocity profiles are shown in Figure 3. For reference the solution on a large-domain is shown in solid black line with the label NSL. The other curves represent the streamwise  $u_1$  and vertical  $u_2$  components of the total velocity as a function of the iteration number between the viscous potential and total velocity on the reduced domain. The velocity profiles are taken in the transverse direction ( $z$ ) at two different locations. It is observed that the algorithm converges in about five iterations.

**Preliminary Free-Surface Flow Results** First results for free-surface flow are computed for the Wigley hull at Froude number 0.4. Figure 4 shows the profile of the streamwise velocity on a longitudinal cut located  $0.625B$  from centerline at a depth of  $0.2T$ . The total velocity on the large domain is shown with a black line and labeled  $u$ . The viscous potential for the double-body solution is shown as  $\partial_x\varphi_{db}$ , and the viscous potential that incorporates wave effects only within the rotational region is labeled as  $\partial_x\varphi'$ . Finally, the inviscid potential with linear wave boundary conditions is shown in the red line and labeled  $\partial_x\phi_{lin}$ .

Work is currently underway on computing a full viscous potential on a free-surface domain. We plan on presenting the newer results at the workshop.

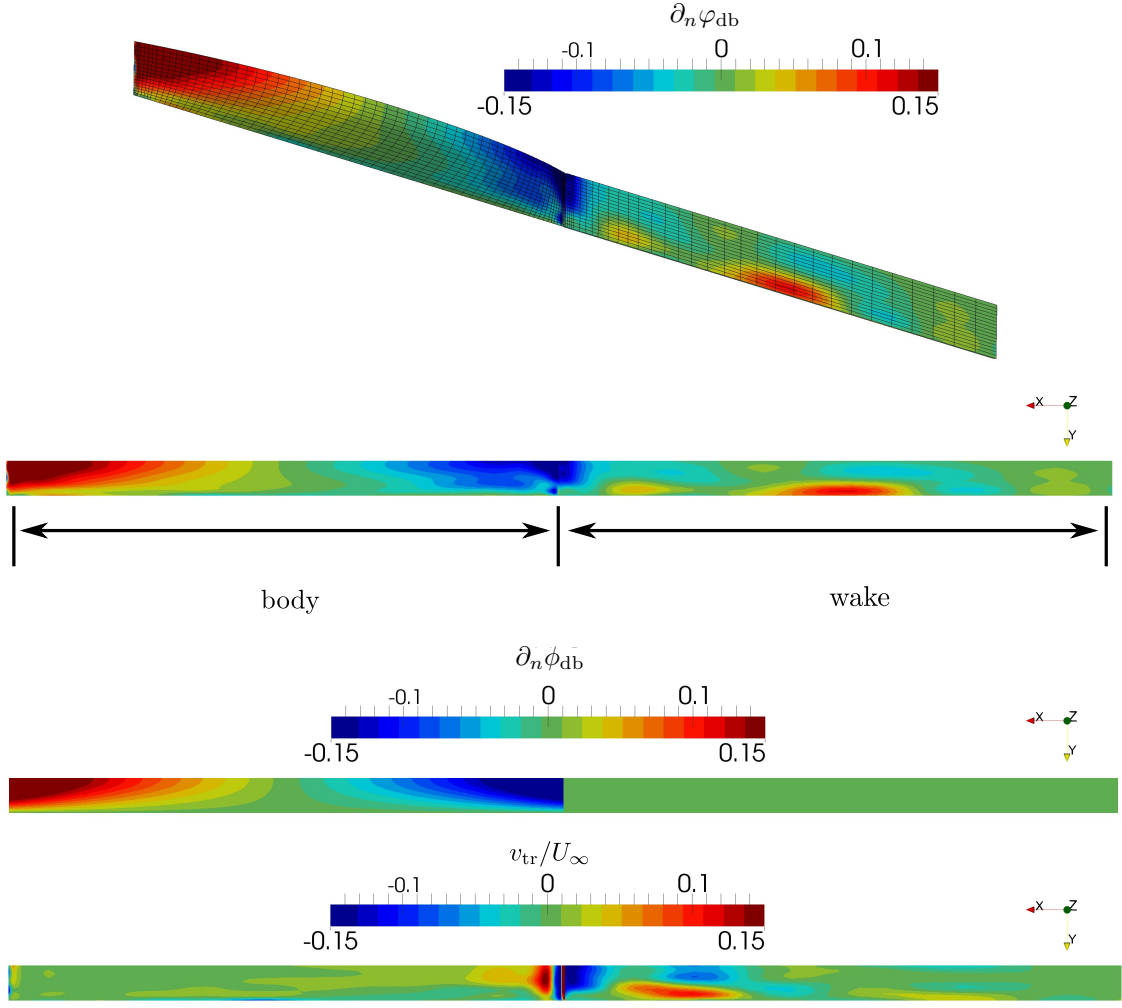


Figure 1: Results for double-body flow. (top) BEM discretization and viscous-potential body-boundary condition on hull and wake. (middle) inviscid body-boundary condition on hull and wake. (bottom) Transpiration velocity on hull and wake as seen from side.

**Acknowledgements** The authors would like to gratefully acknowledge the U.S. Office of Naval Research for the support of this work under contracts N00014-13-1-0558, N00014-14-1-0577, and N00014-16-1-2971.

## REFERENCES

- [1] E. Campana, A. Di Mascio, P. Esposito, and F. Lalli. Viscous-inviscid coupling in free surface ship flows. *International Journal for Numerical Methods in Fluids*, 21:699–722, 1995.
- [2] Y. Chen and K. J. Maki. A velocity decomposition approach for three-dimensional unsteady flow. *European Journal of Mechanics - B/Fluids*, 62:94 – 108, 2017.
- [3] Y. Chen, K. J. Maki, and W. J. Rosemurgy. A velocity decomposition approach for unsteady external flow. In *ASME 34th International Conference on Ocean, Offshore and Arctic Engineering OMAE 2015*, St. John’s, Newfoundland and Labrador, Canada, May 31-June 5 2015.
- [4] D. O. Edmund, K. J. Maki, and R. F. Beck. A velocity-decomposition formulation for the incompressible Navier–Stokes equations. *Comput Mech*, 52:669–680, 2013.
- [5] S.A.G. Joncquez, H. Bingham, P. Andersen, and D. Kring. Validation of added resistance computations by a potential-flow boundary-element method. In *27th Symposium on Naval Hydrodynamics*, 2008.
- [6] W. J. Rosemurgy, R. F. Beck, and K. J. Maki. A velocity decomposition formulation for 2d steady incompressible lifting problems. *European Journal of Mechanics B/Fluids*, 58:70–84, 2016.

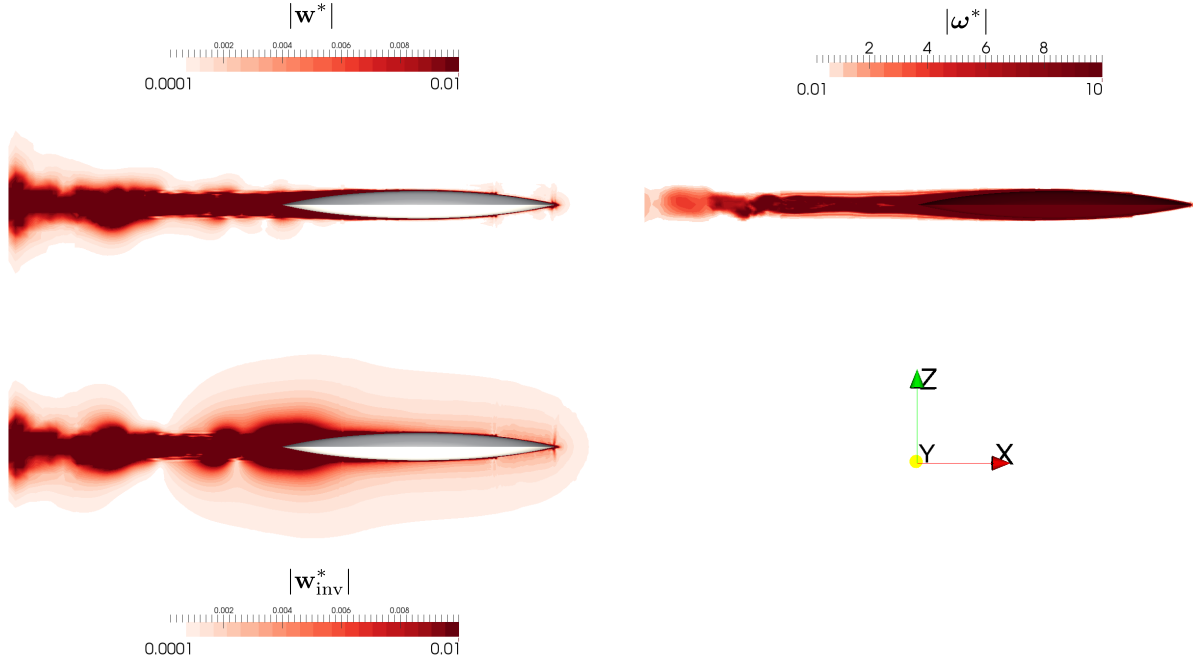


Figure 2: Double-body flow. (*top-right*) contours of dimensionless vorticity. (*top-left*) contours of dimensionless vortical velocity using *viscous* potential. (*bottom*) contours of dimensionless vortical velocity using *inviscid* potential.

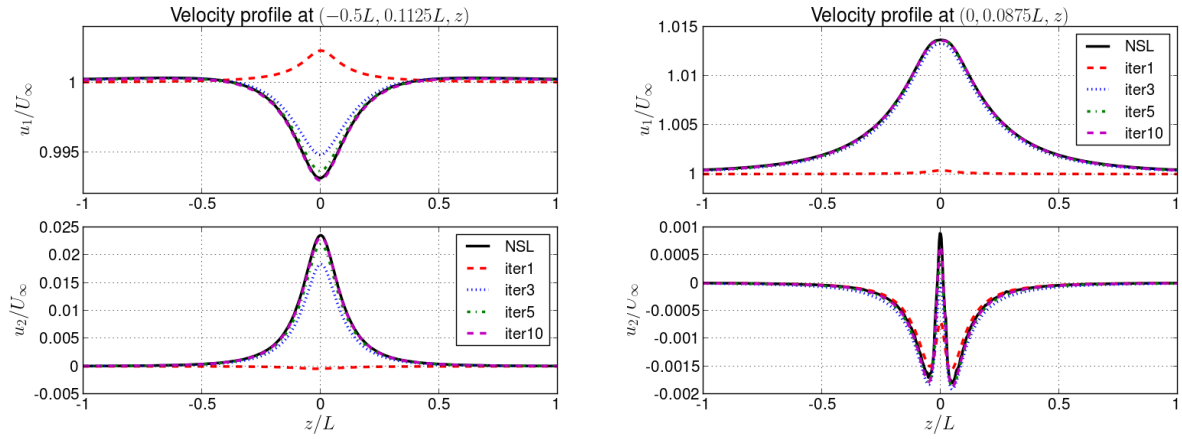


Figure 3: Velocity profiles for double-body flow.

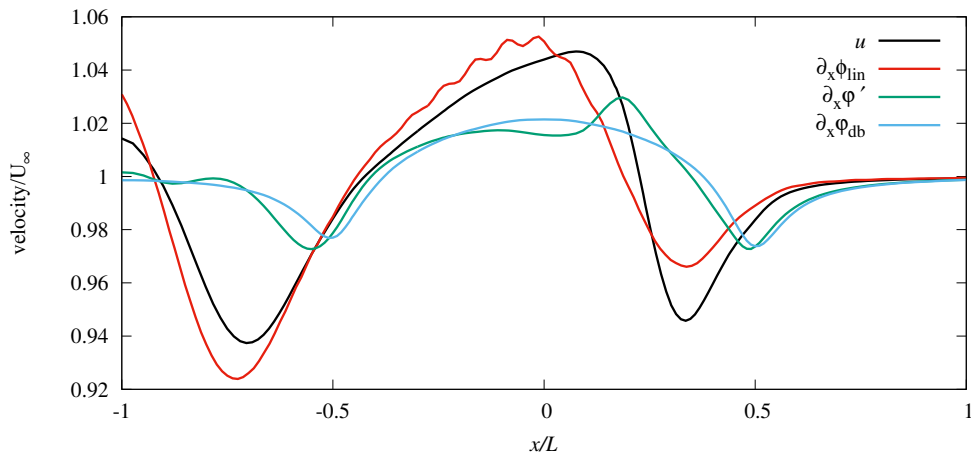


Figure 4: Velocity profile for free-surface flow around the Wigley Hull.